

Abbreviations

pic	picolinamide
sal	salicylic acid
man	S-mandelic acid
mal	malonic acid
suc	succinic acid
fum	fumaric acid
glu	glutaric acid
adi	adipic acid
TGA	thermogravimetric analysis
DSC	differential scanning calorimetry
XRPD	X-ray powder diffraction
VTXRD	variable temperature (powder) X-ray diffraction
PAW	projector augmented wave
PBE	Perdew–Burke–Ernzerhof
DFT-D	density functional theory with dispersion correction
VASP	Vienna <i>ab initio</i> Simulation Package

1.0 Experimental sections

1.1 Preparation of cocrystals

A. Temperature cycling slurry

0.4 mmol of **fum**, **suc** and **adi**, and 0.8 mmol of **glu** and **adi** were weighed separately in five different vials. 0.8 mmol of **pic** was weighed and added to each vial. The physical mixtures were suspended in ethanol. The temperature cycle profile was controlled by a HEL PolyBLOCK PB4: heating from 16 to 45 °C at a rate 0.5 °C min⁻¹ and cooling from 45 to 16 °C at a rate 0.2 °C min⁻¹. The cycles continued for more than 24 hours.

B. Vapour diffusion

0.4 mmol of **mal** and 0.8 mmol **sal** and **man** were weighed separately in three different vials. Equimolar **pic** was weighed and added to each vial. The physical mixtures were dissolved in hot ethyl acetate. Each vial was then placed in a larger capped vial containing isohexane (antisolvent). Isohexane vapour was allowed to diffuse slowly into the concentrated ethyl acetate solution.

The solids obtained from both methods were centrifuged at 13,000 rotations per minute for 10 minutes. The residues were dried in a vacuum oven 40 °C and 10 mBar.

1.2 TGA

Each analysis was performed using a TA Instruments Thermogravimetric analyzer TGA5000. The sample was placed on a tared open aluminium pan and its weight was recorded accurately. The TGA thermogram was recorded as follows: the sample was loaded into the furnace, the temperature equilibrated at 40 °C and heated to 300 °C at a heating rate of 10 °C min⁻¹, under a flow of nitrogen at 25 mL min⁻¹. The instrument was calibrated for temperature with nickel and aluminum, and calibrated for weight with a 100 mg standard.

1.3 DSC

The DSC analysis was performed using a TA Instruments DSC Q2000. Accurately weighed samples were placed into crimped aluminium pans. An empty sample pan was used as reference. The DSC thermogram was recorded as follow: the temperature of the apparatus was adjusted to about 40°C, and heated to 300°C at an heating rate of 10°C min⁻¹, under a nitrogen flow of 50 mL min⁻¹.The instrument was calibrated for temperature and enthalpy with Indium, at least 99.9999 % pure.

1.4 Raman

The Raman spectra were recorded by a Renishaw inVia Raman spectrometer which operated with 785 nm laser excitation. 10 seconds laser exposure time and 3 spectral accumulations were acquired. The spectral range and spectral resolution were 100 – 3200 cm^{-1} and 4 cm^{-1} respectively. For **pic**, a 20 seconds laser exposure was used. For **1:1 pic:mal**, the sample was photo bleached for 60 seconds prior to each acquisition. An internal wavelength calibration was performed using a standard wafer Si (001) with Raman scattering band at $520.0 \pm 0.5 \text{ cm}^{-1}$ for the correction of spectral offset with a mixture of Ar-Ne as calibration source.

1.5 XRPD and VTNRD

A monochromatic $K\alpha$ radiation of wavelength 1.54 Å was generated from the Cu anode in a Bruker GADD D8 Discover Diffractometer. The sample was placed on a glass slide and centered in the X-ray beam. The distance between the sample and the detector was 30 cm. The diffractogram in 2θ range from 7° to 39° was recorded at room temperature in two frames. The VTNRD was carried out only for the **1:1 pic:adi** cocrystal. The powder was mounted on a capped hot stage controlled by Anton Parr TCU100 Temperature Control Unit. The temperature was sequentially set at room temperature, 100 °C, 105 °C and 110 °C during the heating phase, and then at 45 °C and 20 °C during the cooling phase. The diffractogram was recorded after equilibrating the sample at each targeted temperature for two minutes.

A separate VTNRD experiment for **1:1 pic:adi** was conducted at Goethe University. The sample was filled into an open glass capillary with 0.7 mm diameter. Data were recorded in transmission mode on a STOE Stadi-P diffractometer equipped with a Ge(111) monochromator and a position-sensitive detector. Cu- $K_{\alpha 1}$ radiation ($\lambda = 1.5406 \text{ Å}$) was used. A 2θ range of 5 to 40° was selected. The sample was heated by a nitrogen stream using an Oxford Cryosystem device. For each temperature level, the sample was heated with 6 K/min until the corresponding temperature was reached, then kept at this temperature for 10 minutes, and subsequently measured at this temperature for about 2 hours, before going to the next temperature. Finally the sample was cooled to room temperature and measured again.

1.6 SXD

Intensity data were collected at 100 K on a Bruker AXS three-circle diffractometer with graphite-monochromated Cu(K_{α})-radiation from a fine focus sealed tube generator and a

Smart 6000 CCD detector using the SMART software (Bruker AXS (2003)). 5 ω -scans at different ϕ -positions were performed to ensure appropriate data redundancy. Data processing and global cell refinement were performed with Saint (Bruker AXS (2005)). A semi-empirical absorption correction was applied, based on the intensities of symmetry-related reflections measured at different angular settings.

1.7 DFT-D calculations

The lattice energy minimisations were performed using the GRACE software package, version 2.0.¹ This software calculates DFT energies using VASP 5.2^{2,3} and implements a correction for the van der Waals energy.⁴ Projector augmented wave (PAW) potentials and the PBE exchange-correlation functional with the Vosko, Wilk, and Nusair interpolation formula were used for DFT calculations. The plane-wave cut-off energy was set at 520 eV. The k -point spacing in the Brillouin zone was approximately 0.7 \AA^{-1} . The wave function convergence level was $0.5 \times 10^{-6} \text{ kcal mol}^{-1}$ per atom. The van der Waals correction is expressed as a pair-wise sum over all atoms. The C6 coefficients of the van der Waals correction have been parameterised using experimental dipole oscillator strength distribution data. Minimisations were complete when the change in lattice energy was no more than $0.25 \times 10^{-3} \text{ kcal mol}^{-1}$ per atom, atomic displacements were no more than $3 \times 10^{-3} \text{ \AA}$, and maximum atomic forces were no more than $0.7 \text{ kcal \AA}^{-1} \text{ mol}^{-1}$ per atom.

The crystal packing similarity tool in Mercury CFC 3.1⁵ was used to calculate the root-mean-squared deviations in atomic coordinates with a 16 molecule comparison between the experimental and the optimised structures, excluding hydrogen atoms.

2.0 Results

2.1 TGA and DSC

The TGA and the DSC thermograms are labelled using dotted and solid lines respectively.

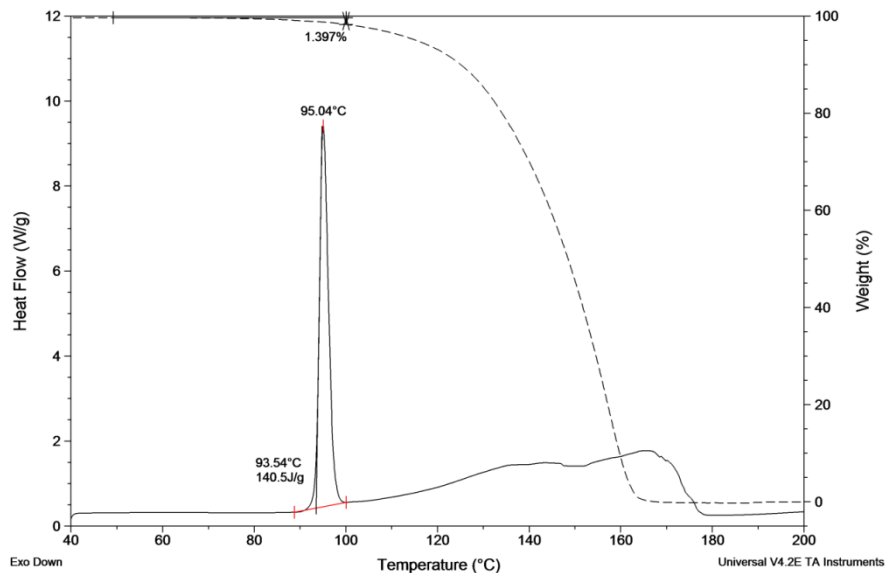


Fig. S2.1a Solids obtained from a concentrated solution consisting of 1:1 **pic** and **sal** after vapour diffusion experiment.

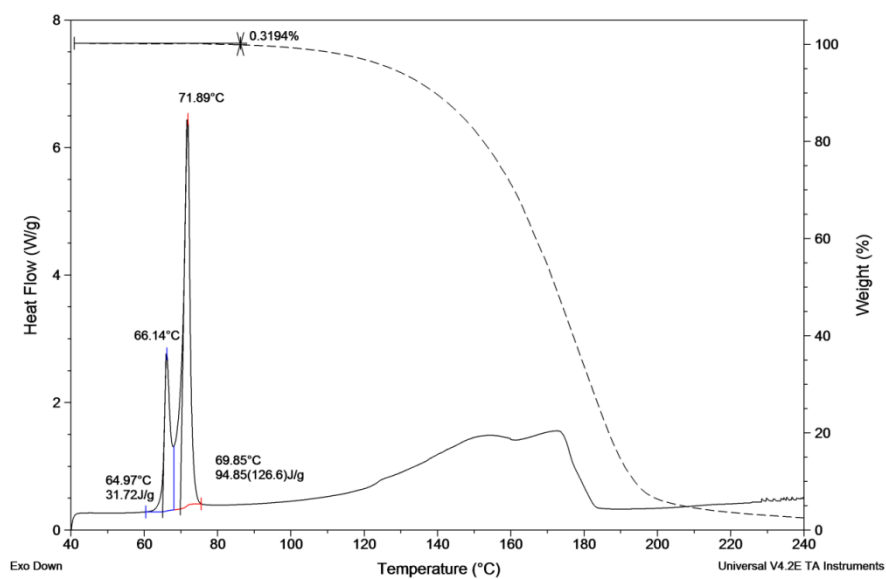


Fig. S2.1b Solids obtained from a concentrated solution consisting of 1:1 **pic** and **man** after vapour diffusion experiment.

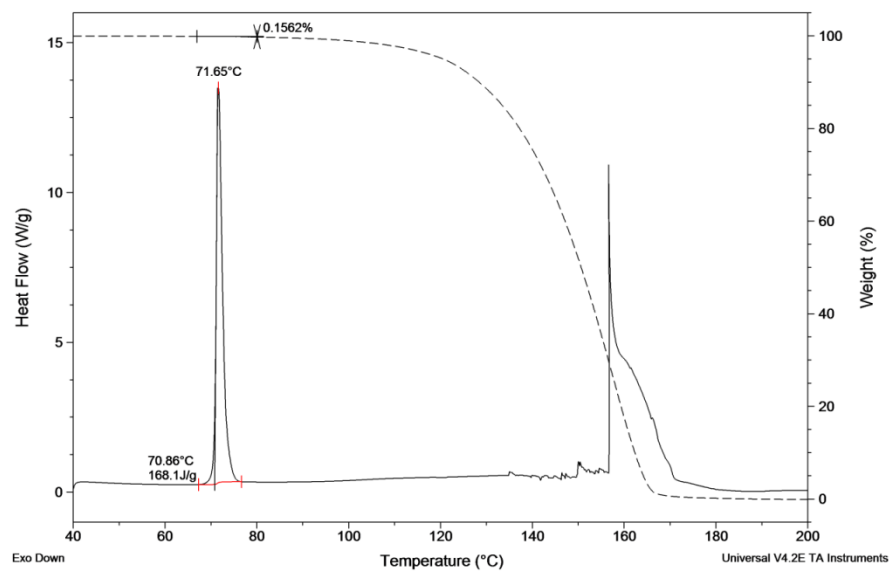


Fig. S2.1c Solids obtained from a concentrated solution consisting of 1:1 **pic** and **mal** after vapour diffusion experiment.

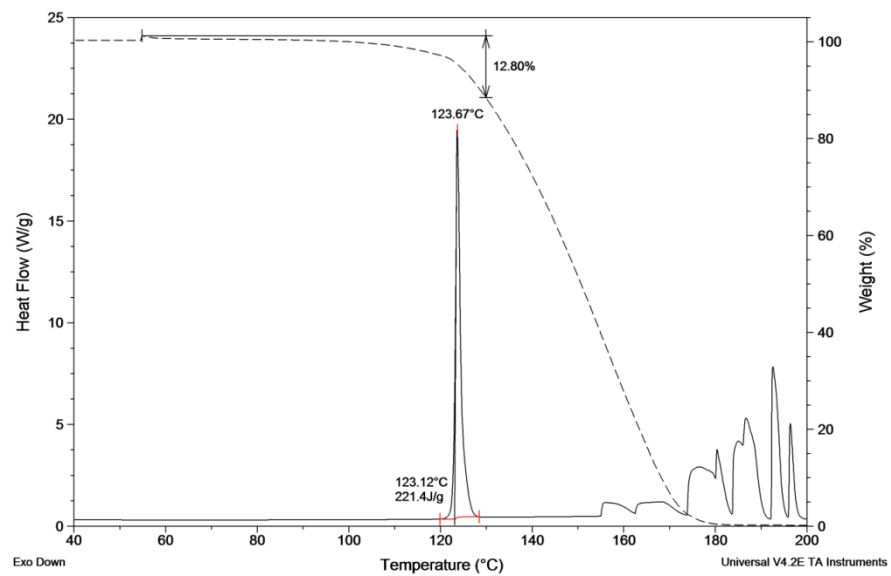


Fig. S2.1d Solids in a slurry consisting of 2:1 **pic** and **suc** after temperature cycling.

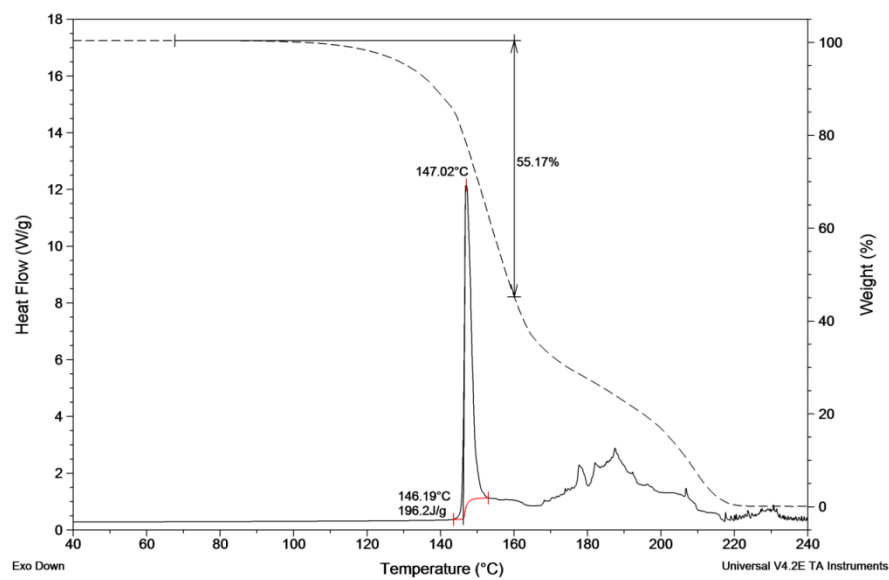


Fig. S2.1e Solids in a slurry consisting of 2:1 **pic** and **fum** after temperature cycling.

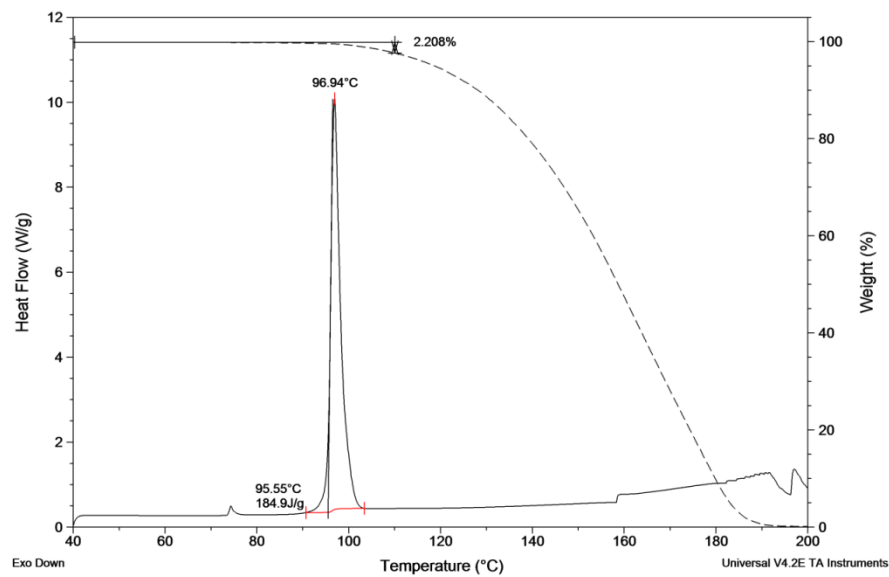


Fig. S2.1f Solids in a slurry consisting of 1:1 **pic** and **glu** after temperature cycling. SXD experiment confirmed that the sample contained **2:1 pic:glu** cocrystal instead.

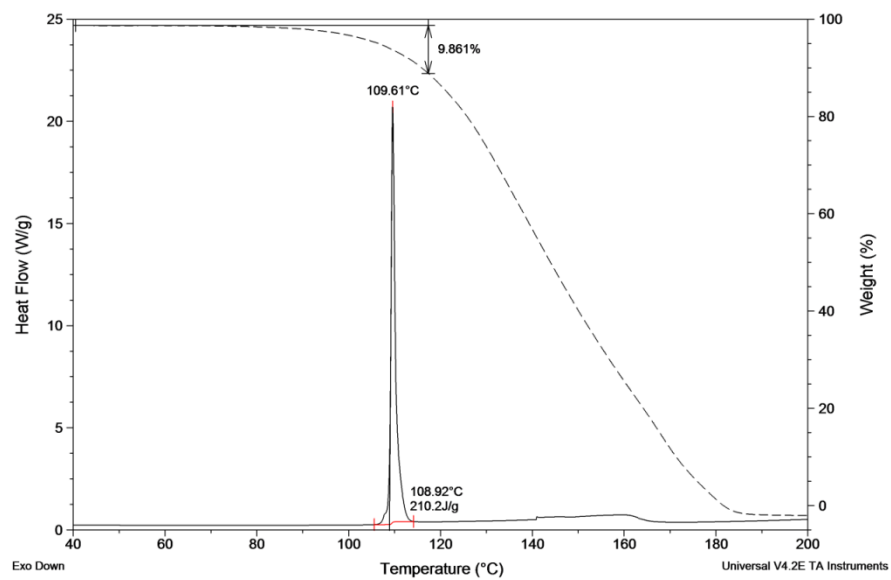


Fig. S2.1g Solids in a slurry consisting of 2:1 **pic** and **adi** after temperature cycling.

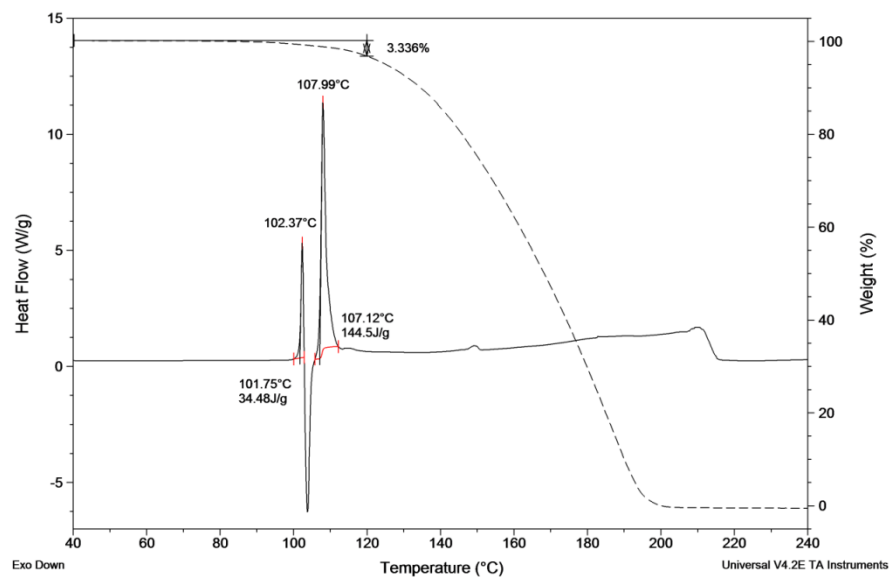


Fig. S2.1h Solids in a slurry consisting of 1:1 **pic** and **adi** after temperature cycling.

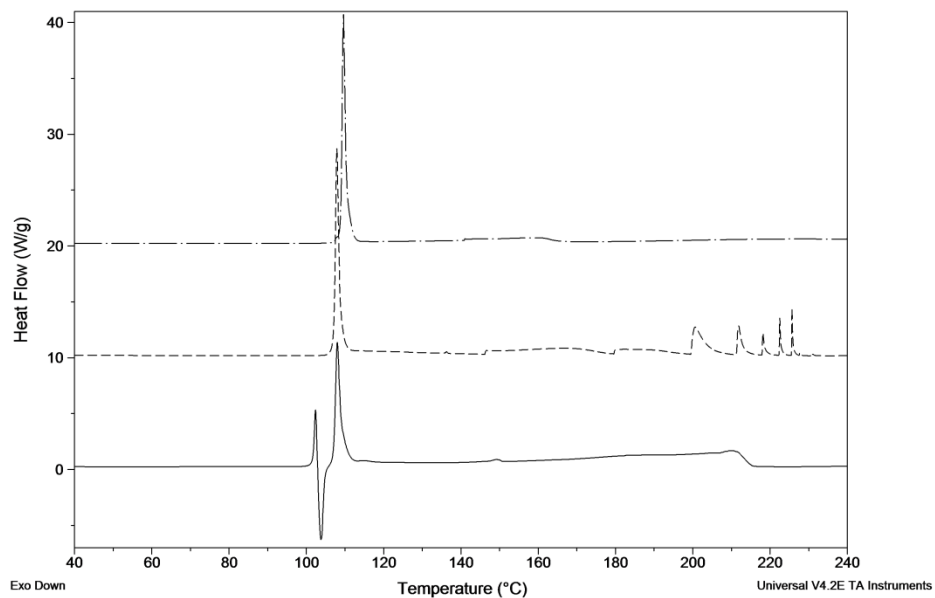


Fig. S2.1i The DSC thermograms of **2:1 pic:adi** (top), solids obtained by post heating **1:1 pic:adi** on HSM (middle) and **1:1 pic:adi** (bottom). The result suggests a temperature induced conversion from **1:1 pic:adi** to **2:1 pic:adi**.

2.2 Raman

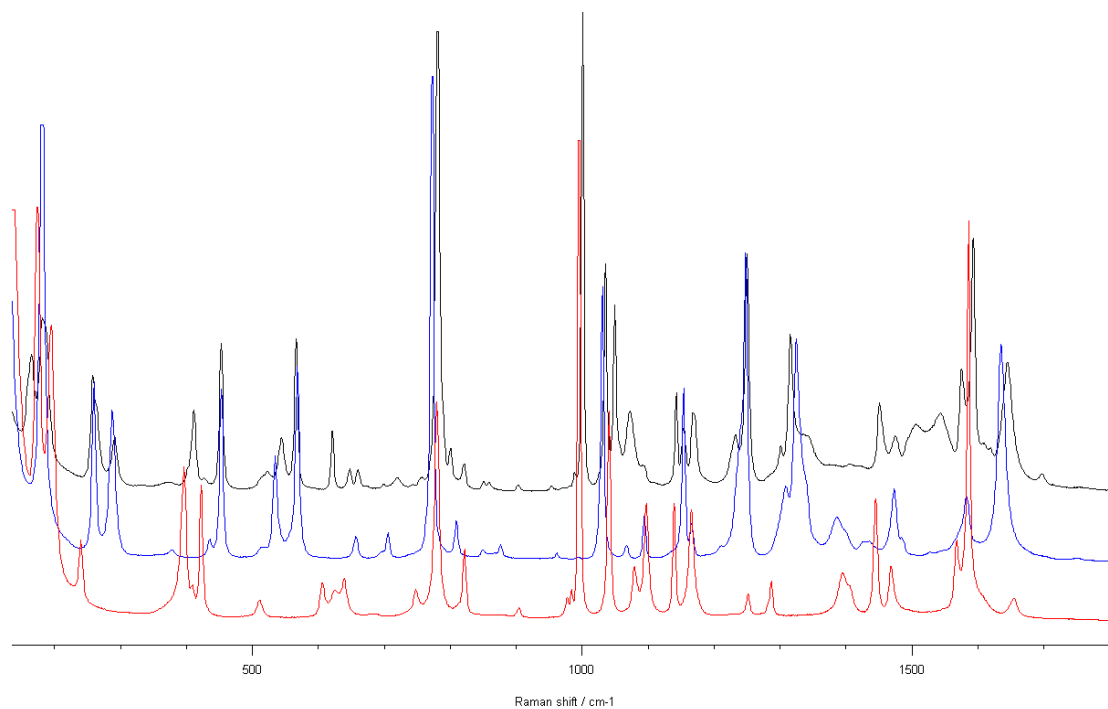


Fig. S2.2a Raman spectra of the solids obtained from a concentrated solution consisting of 1:1 **pic** and **sal** after vapour diffusion experiment (black), **sal** (blue) and **pic** (red).

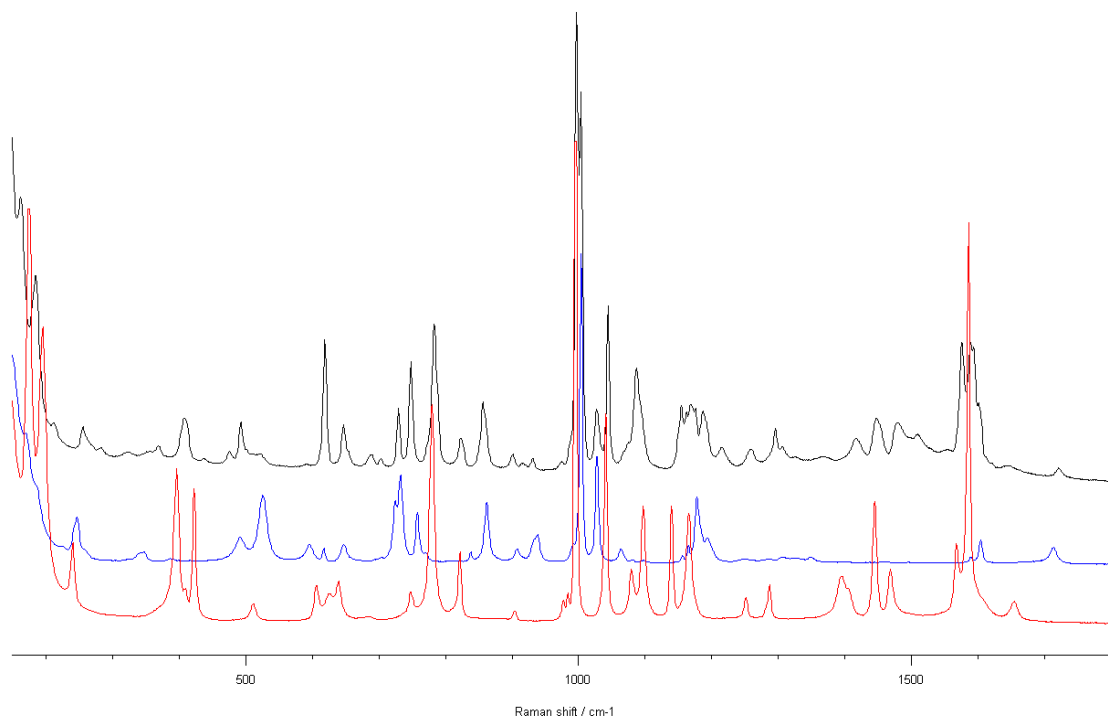


Fig. S2.2b Raman spectra of the solids obtained from a concentrated solution consisting of 1:1 **pic** and **man** after vapour diffusion experiment (black), **man** (blue) and **pic** (red).

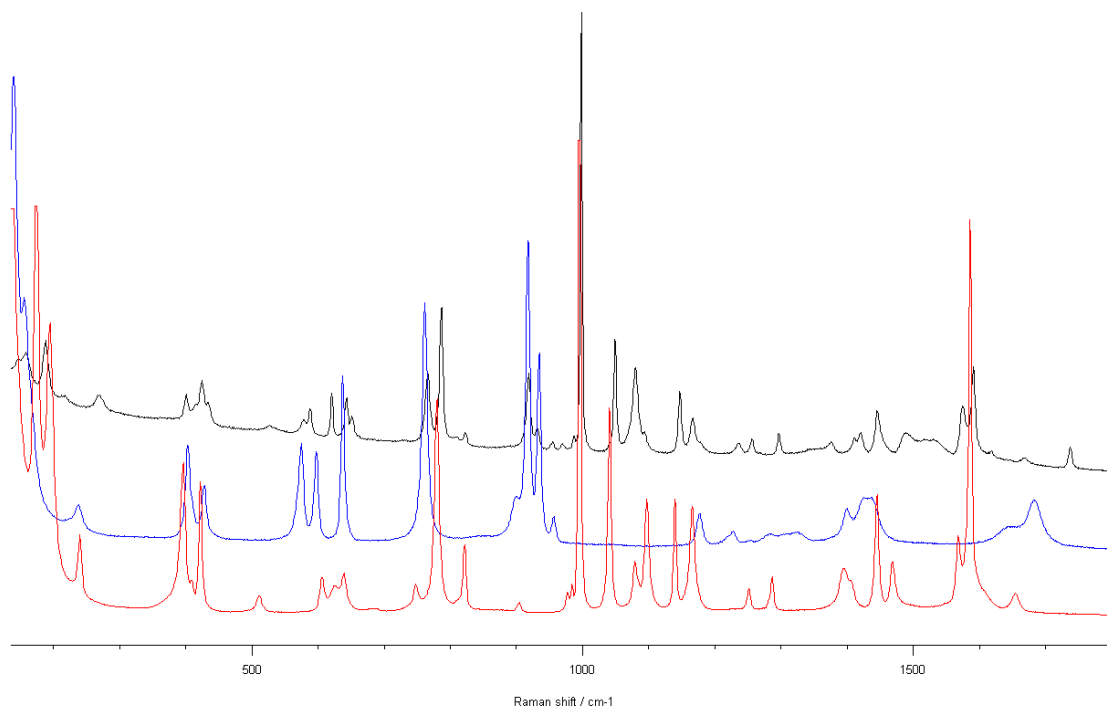


Fig. S2.2c Raman spectra of the solids obtained from a concentrated solution consisting of 1:1 **pic** and **mal** after vapour diffusion experiment (black), **mal** (blue) and **pic** (red).

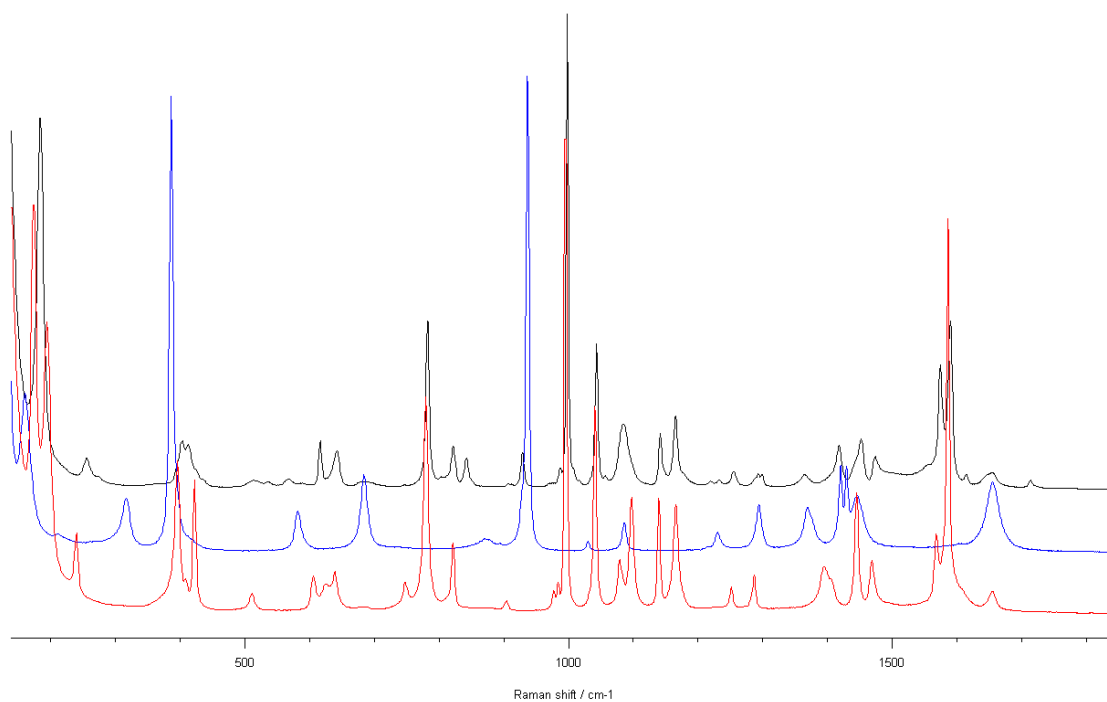


Fig. S2.2d Raman spectra of the solids in a slurry consisting of 1:1 **pic** and **suc** after temperature cycling (black), **suc** (blue) and **pic** (red).

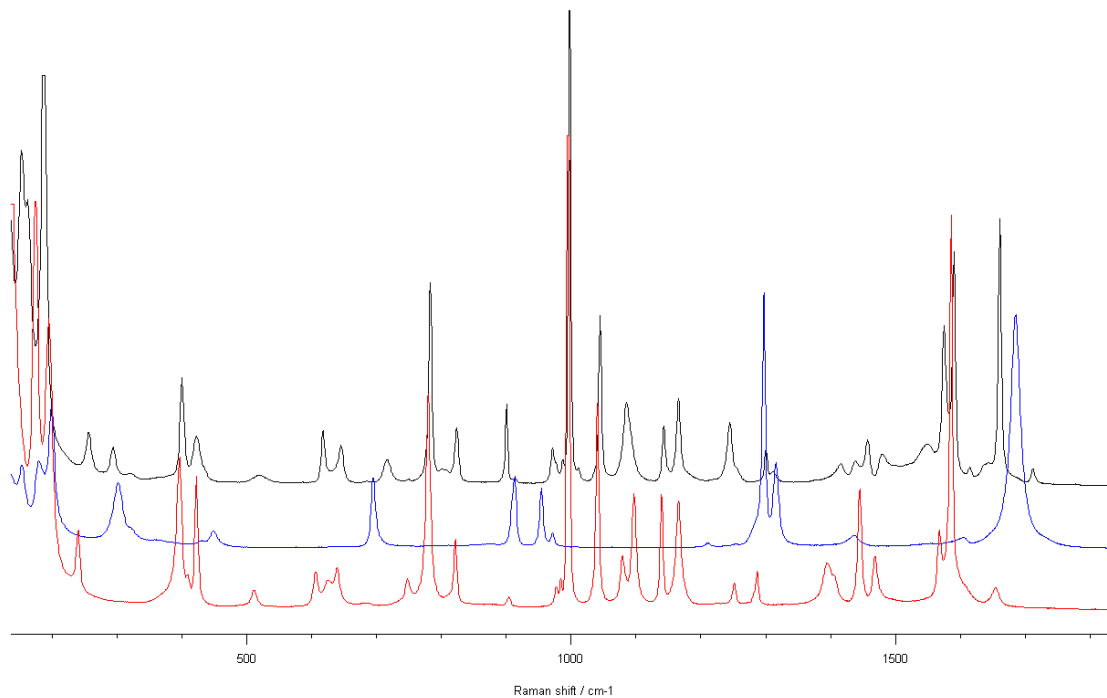


Fig. S2.2e Raman spectra of the solids in a slurry consisting of 1:1 **pic** and **fum** after temperature cycling (black), **fum** (blue) and **pic** (red).

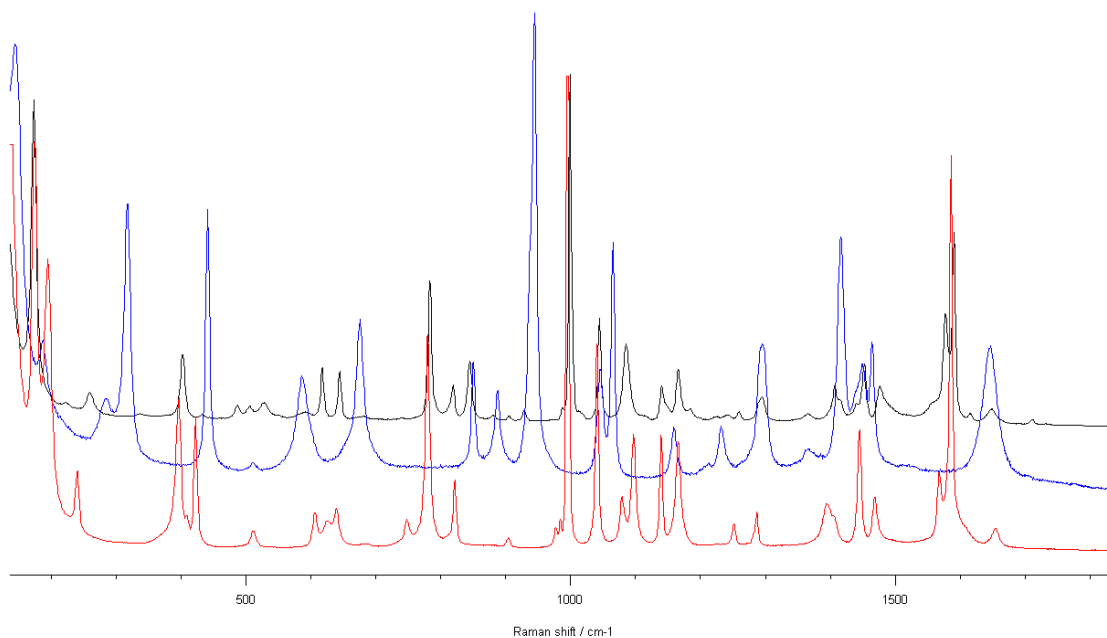


Fig. S2.2f Raman spectra of the solids in a slurry consisting of 1:1 **pic** and **glu** after temperature cycling (black), **glu** (blue) and **pic** (red). SXD experiment confirmed that the sample contained **2:1 pic:glu** cocrystal instead.

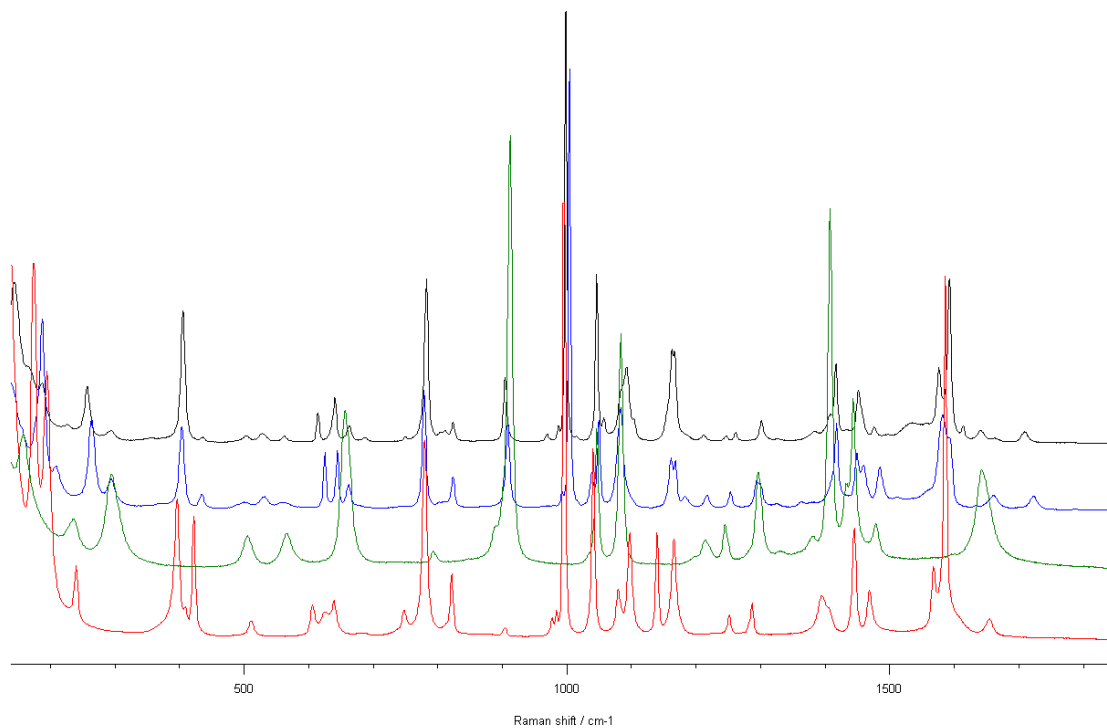


Fig. S2.2g Raman spectra of the solids in a slurry consisting of 2:1 **pic** and **adi** after temperature cycling (black), the solids in a slurry consisting of 1:1 **pic** and **adi** (blue), **adi** (green) and **pic** (red).

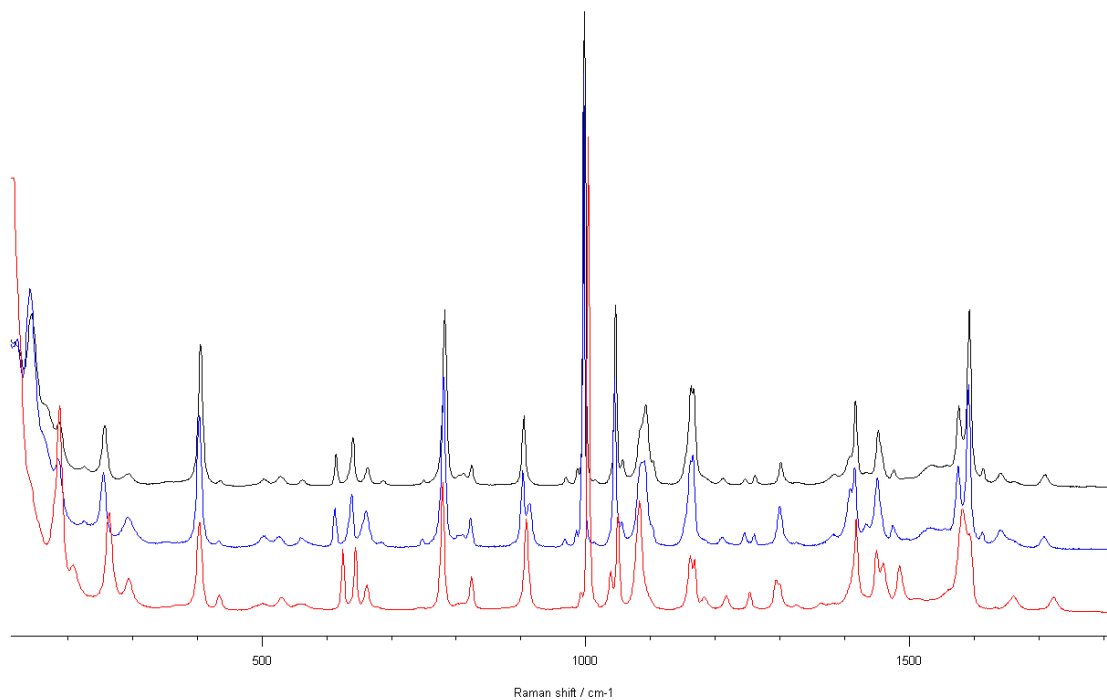


Fig. S2.2h The Raman spectra of 2:1 **pic:adi** (black), the solid obtained by recrystallising the melt of 1:1 **pic:adi** (blue) and 1:1 **pic:adi** (red).

2.3 XRPD and VTXRD

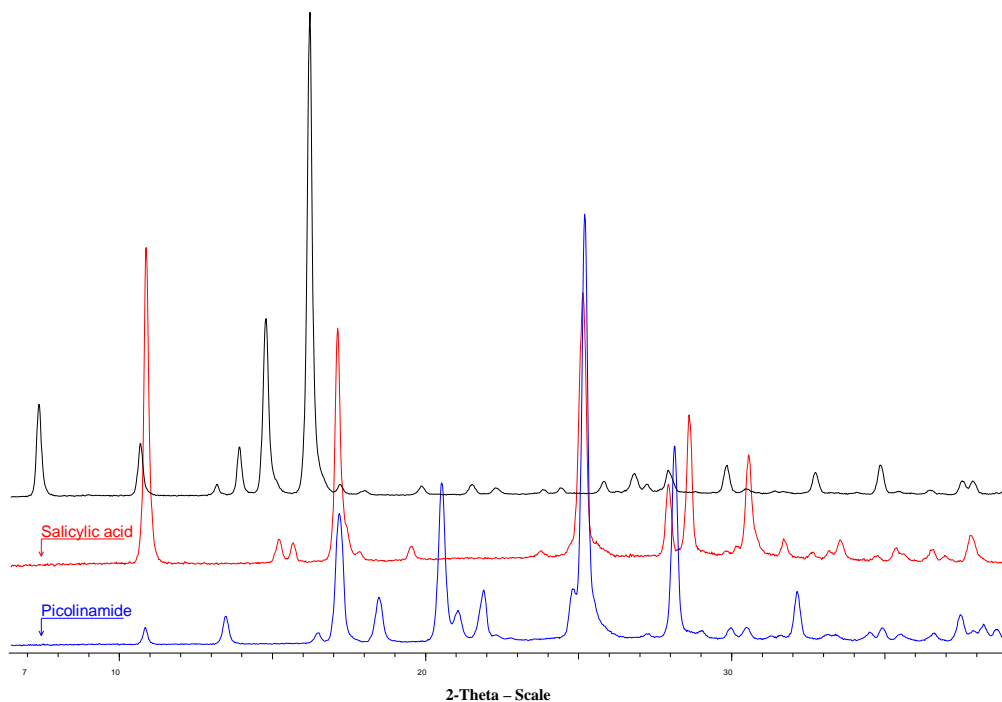


Fig S2.3a Diffractograms of the solids obtained from a concentrated solution consisting of 1:1 **pic** and **sal** after vapour diffusion experiment (black), **sal** (red) and **pic** (blue).

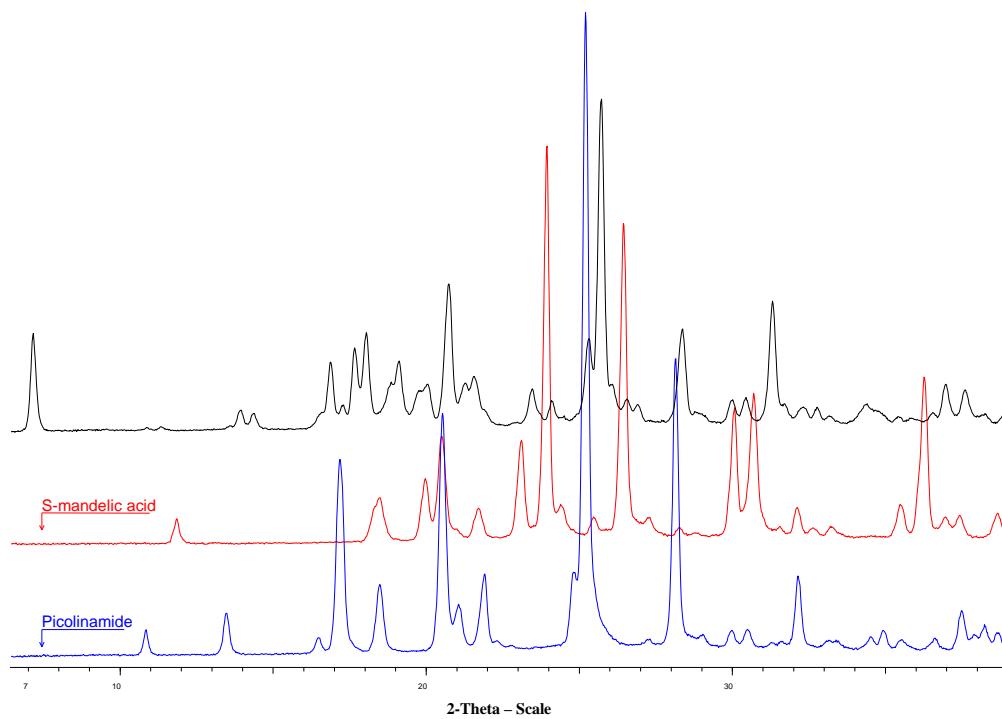


Fig. S2.3b Diffractograms of the solids obtained from a concentrated solution consisting of 1:1 **pic** and **man** after vapour diffusion experiment (black), **man** (red) and **pic** (blue).

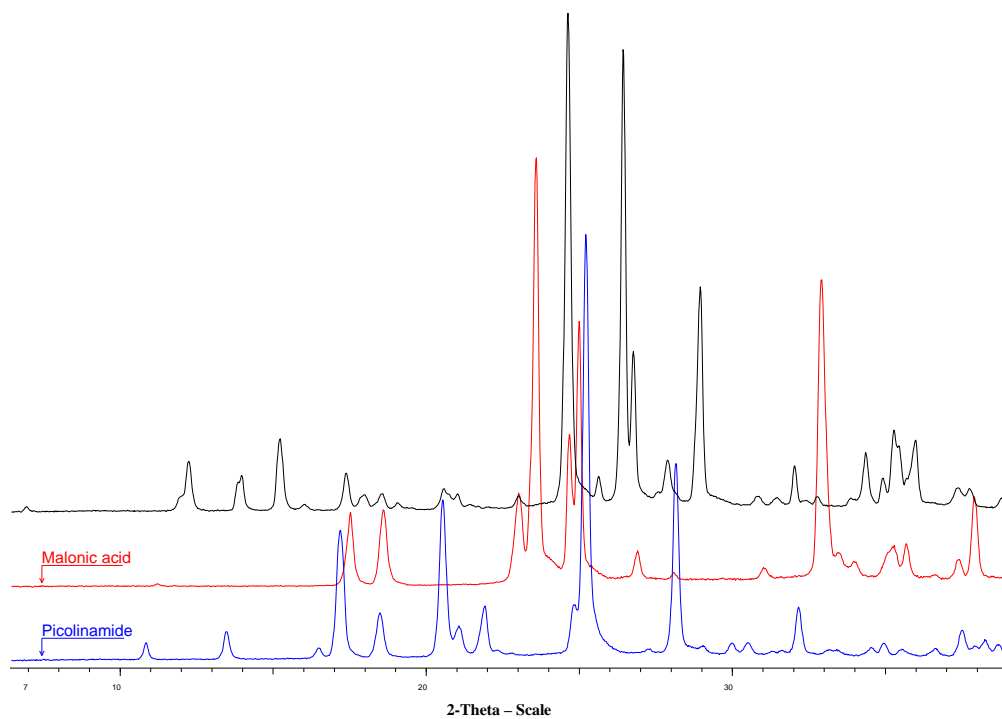


Fig. S2.3c Diffractograms of the solids obtained from a concentrated solution consisting of 1:1 **pic** and **mal** after vapour diffusion experiment (black), **mal** (red) and **pic** (blue).

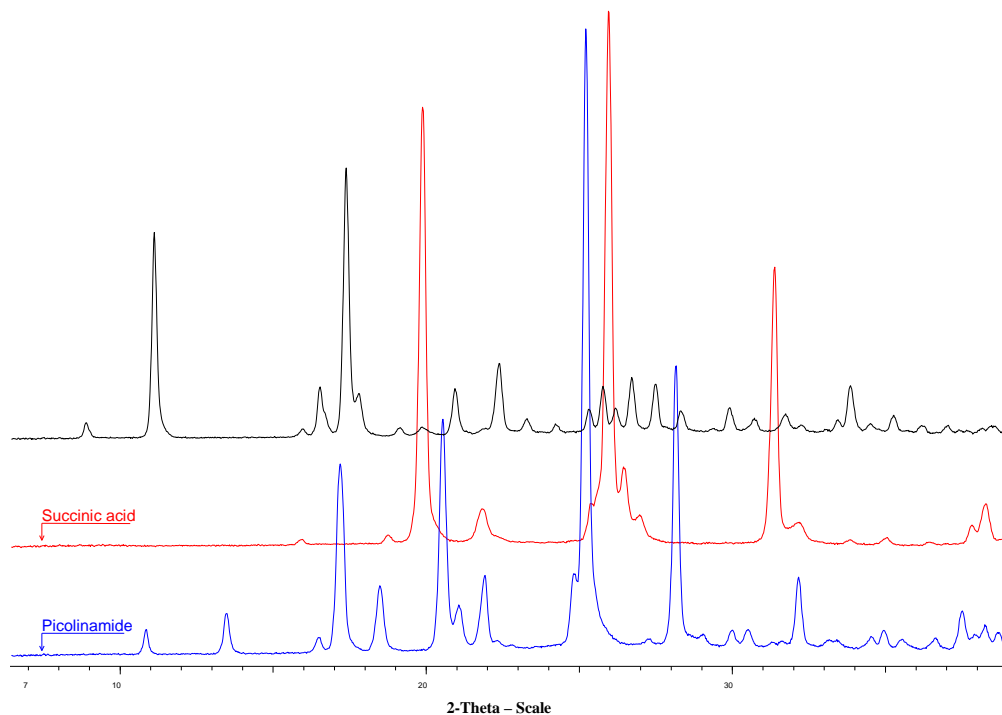


Fig. 2.3d Diffractograms of the solids in a slurry consisting of 2:1 **pic** and **suc** after temperature cycling (black), **suc** (red) and **pic** (blue).

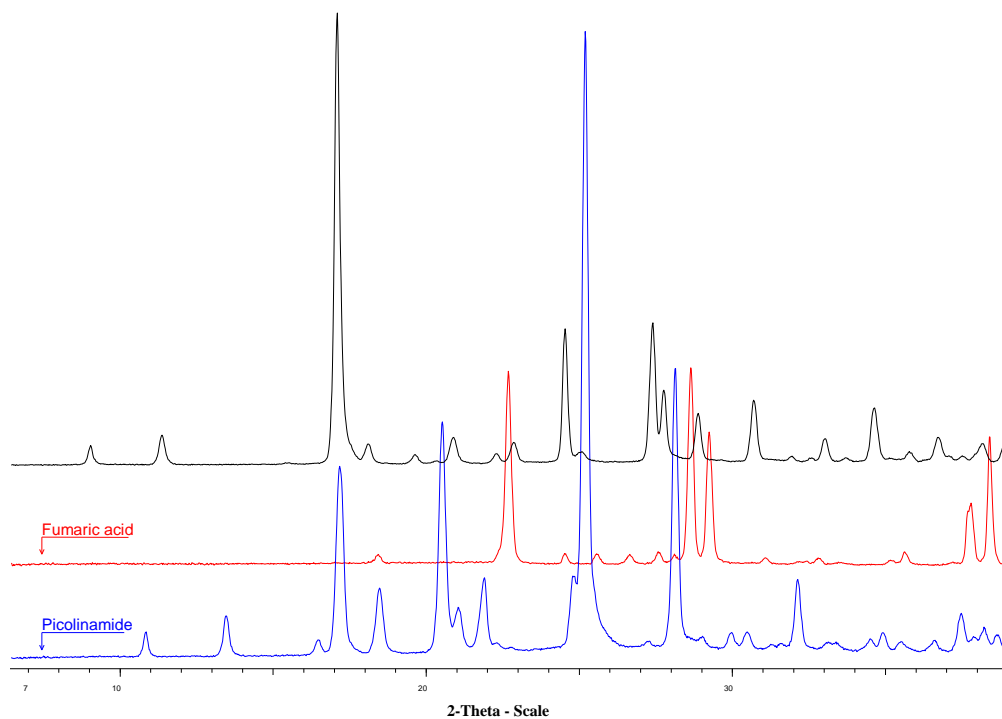


Fig. S2.3e Diffractograms of the solids in a slurry consisting of 2:1 **pic** and **fum** after temperature cycling (black), **fum** (red) and **pic** (blue).

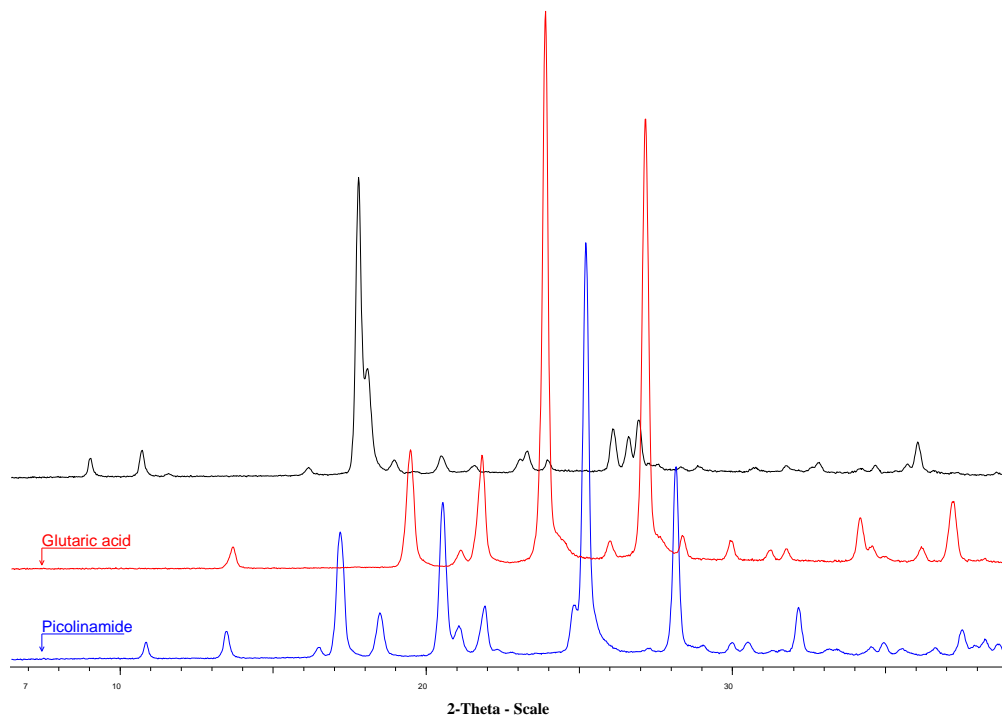


Fig. S2.3f Diffractograms of the solids in a slurry consisting of 1:1 **pic** and **glu** after temperature cycling (black), **glu** (red) and **pic** (blue). SXD experiment confirmed that the sample contained **2:1 pic:glu** cocrystal instead.

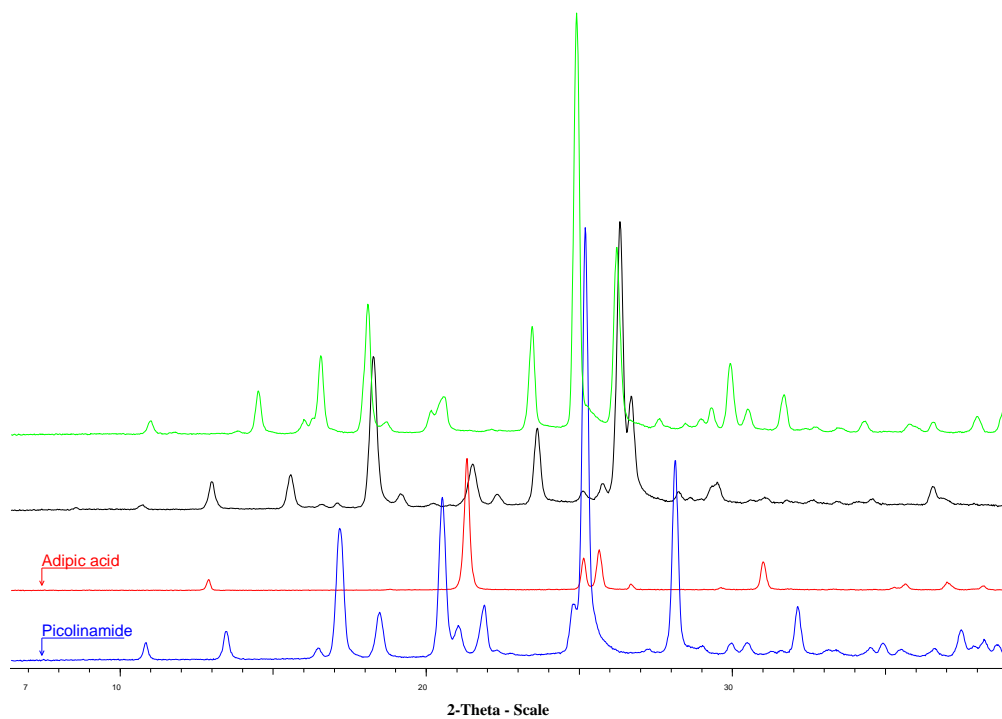


Fig. S2.3g Diffractograms of the solids in a slurry consisting of 2:1 **pic** and **adi** after temperature cycling (green), the solids in a slurry consisting of 1:1 **pic** and **adi** (black), **adi** (red) and **pic** (blue).

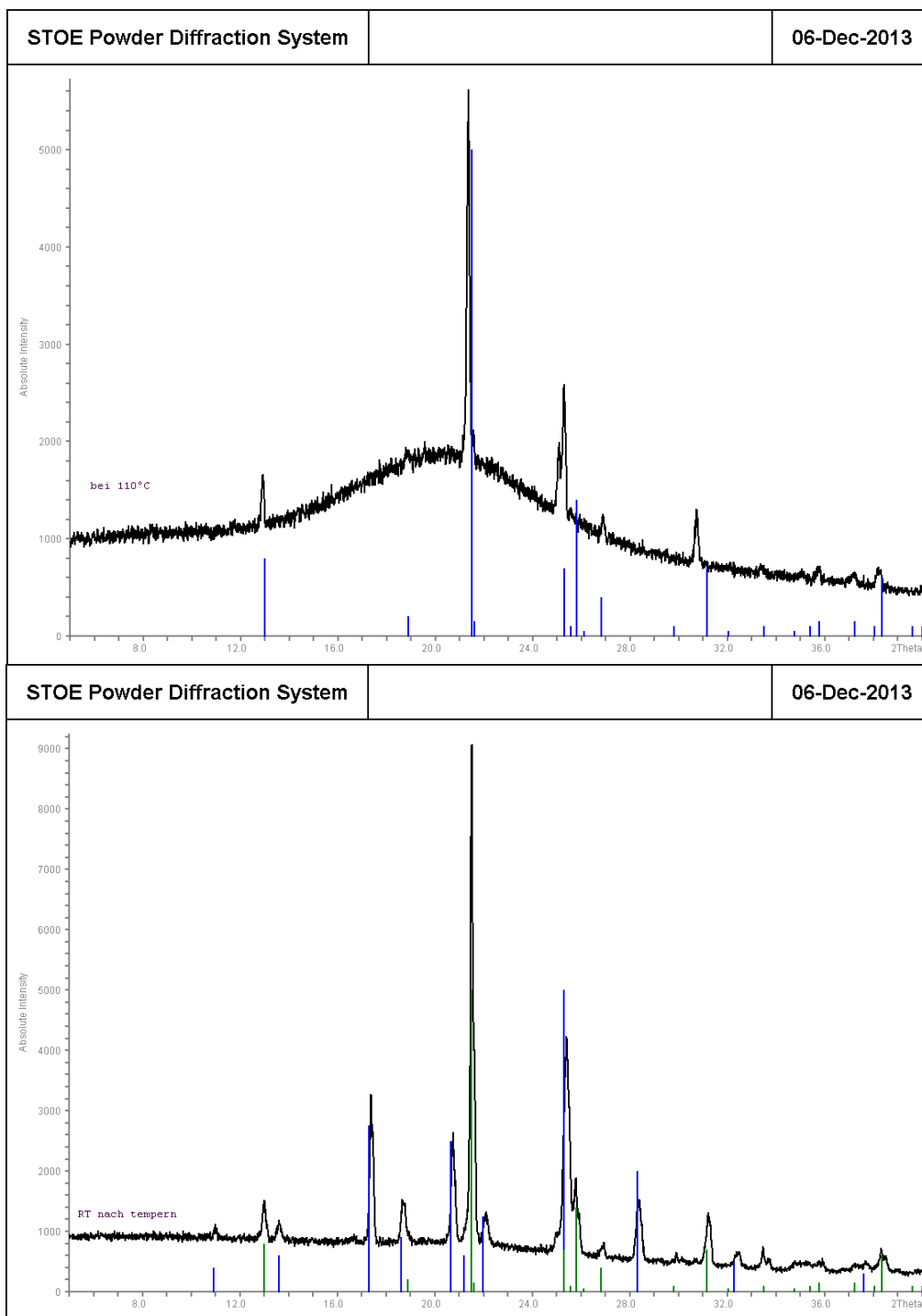


Fig. S2.3h The VT-XRD results at Goethe University: **(Top)** X-ray powder pattern measured at 110°C. The blue vertical lines show the simulated reflections of adipic acid. The lines of the experimental diagram are shifted to smaller angles (i.e. larger d-values) due to the thermal expansion of the lattice. **(bottom)** X-ray powder pattern after cooling to room temperature. Green: Simulated reflections of adipic acid. Blue: Simulated reflections of picolinamide.

2.4 DFT-D calculations

Table S1: DFT-D lattice energies of the pure coformers of the picolinamide cocrystals found in this study. The most stable polymorph of each compound is given in bold.

Compound	CSD code ^[a]	Polymorph type	$E_{\text{DFT-D}}^{\text{[b]}}$ (kcal mol ⁻¹)	RMSD ^[c] (Å)
picolinamide	PICAMD	form II	-2326.12	0.091
	This study	form I	(+0.27)	0.065
salicylic acid	SALIAC16	–	-2473.22	0.155
mandelic acid	DLMAND03	orthorhombic (racemic)	-2845.33	0.246
	DLMAND02	monoclinic (racemic)	(+1.34)	0.095
	FEGHAA	(S-enantiomer)	(+1.59)	0.112
malonic acid	MALNAC03	alpha	-1633.39	0.111
	MALNAC09	beta	(+0.48)	0.157
	MALNAC08	gamma	(+0.48)	0.227
succinic acid	SUCACB07	alpha	-2021.66	0.133
	SUCACB03	beta	(+0.01)	0.136
fumaric acid	FUMAAC	alpha	-1829.03	0.150
	FUMAAC01	beta	(+0.03)	0.214
glutaric acid	GLURAC04	beta	-2404.32	0.141
	GLURAC02	monoclinic III	(+0.01)	0.221
adipic acid	ADIPAC12	form III	-2789.33	0.091
	ADIPAC05	form II	(+0.48)	0.152
	ADIPAC11	form I	(+0.65)	0.063

^[a] CSD = Cambridge Structural Database version 5.34.⁶ ^[b] $E_{\text{DFT-D}}$ is the minimised lattice energy per mole of molecule, calculated by the DFT-D method. Numbers in brackets refer to the energy differences relative to the most stable polymorph, which is given in bold face. ^[c] The root-mean-square deviations in atomic positions after optimisation was calculated by the crystal packing similarity tool in Mercury CFC 3.1⁵ with a 15 molecule comparison to the experimental structures, excluding the hydrogen atoms.

Table S2: DFT-D lattice energies of the experimental and the substituted picolinamide cocrystals and their stabilities relative to the lattice energies of the pure coformer crystals.

Experimental picolinamide cocrystals				
Label	Cocrystal composition	$E_{\text{DFT-D}}^{[a]}$ (kcal mol ⁻¹)	$\Delta E^{[b]}$ (kcal mol ⁻¹)	RMSD ^[c] (Å)
1:1 pic:sal	(picolinamide)·(salicylic acid)	-4800.40	-1.07	0.058
1:1 pic:man	(picolinamide)·(S-mandelic acid)	-5171.65	-0.21	0.093
1:1 pic:mal	(picolinamide)·(malonic acid)	-3960.25	-0.75	0.084
2:1 pic:suc	(picolinamide) ₂ ·(succinic acid)	-6675.71	-1.81	0.065
2:1 pic:fum	(picolinamide) ₂ ·(fumaric acid)	-6483.42	-2.16	0.076
2:1 pic:glu	(picolinamide) ₂ ·(glutaric acid)	-7058.57	-2.02	0.060
2:1 pic:adi	(picolinamide) ₂ ·(adipic acid)	-7443.26	-1.70	0.082
1:1 pic:adi	(picolinamide)·(adipic acid)	-5117.26	-1.81	0.053

Substituted picolinamide cocrystals				
Molecule for substitution	Lattice for substitution	Resulting cocrystal composition	$E_{\text{DFT-D}}^{[a]}$ (kcal mol ⁻¹)	$\Delta E^{[b]}$ (kcal mol ⁻¹)
malonic acid	2:1 pic:suc	(picolinamide) ₂ ·(malonic acid) ^[d]	-6279.15	6.47
	2:1 pic:fum	(picolinamide) ₂ ·(malonic acid) ^[d]	-6276.91	8.71
	2:1 pic:glu	(picolinamide) ₂ ·(malonic acid)	-6285.29	0.33
	2:1 pic:adi	(picolinamide) ₂ ·(malonic acid) ^[d]	-6275.94	9.68
	1:1 pic:adi	(picolinamide)·(malonic acid)	-3959.83	-0.32
succinic acid	1:1 pic:mal	(picolinamide)·(succinic acid)	-4341.79	5.99
	2:1 pic:fum	(picolinamide) ₂ ·(succinic acid)	-6674.93	-1.04
	2:1 pic:glu	(picolinamide) ₂ ·(succinic acid)	-6674.62	-0.73
	2:1 pic:adi	(picolinamide) ₂ ·(succinic acid)	-6671.71	2.19
	1:1 pic:adi	(picolinamide)·(succinic acid)	-4348.24	-0.46
fumaric acid	1:1 pic:mal	(picolinamide)·(fumaric acid)	-4147.60	7.55
	2:1 pic:suc	(picolinamide) ₂ ·(fumaric acid)	-6478.10	3.16
	2:1 pic:glu	(picolinamide) ₂ ·(fumaric acid)	-6477.70	3.56
	2:1 pic:adi	(picolinamide) ₂ ·(fumaric acid)	-6480.00	1.26
	1:1 pic:adi	(picolinamide)·(fumaric acid)	-4154.41	0.74
glutaric acid	1:1 pic:mal	(picolinamide)·(glutaric acid)	-4729.38	1.05
	2:1 pic:suc	(picolinamide) ₂ ·(glutaric acid) ^[d]	-7056.60	-0.05
	2:1 pic:fum	(picolinamide) ₂ ·(glutaric acid) ^[d]	-7053.04	3.51
	2:1 pic:adi	(picolinamide) ₂ ·(glutaric acid) ^[d]	-7050.55	6.00
	1:1 pic:adi	(picolinamide)·(glutaric acid)	-4725.23	5.20
adipic acid	1:1 pic:mal	(picolinamide)·(adipic acid)	-5111.34	4.11
	2:1 pic:suc	(picolinamide) ₂ ·(adipic acid)	-7435.22	6.34
	2:1 pic:fum	(picolinamide) ₂ ·(adipic acid)	-7437.53	4.03
	2:1 pic:glu	(picolinamide) ₂ ·(adipic acid)	-7436.49	5.07

^[a] $E_{\text{DFT-D}}$ is the minimised lattice energy of a cocrystal calculated by the DFT-D method and is expressed in kcal per mole of formula unit which consists of two or more coformer molecules in a fixed stoichiometric ratio. ^[b] ΔE is the calculated energy change in forming a cocrystal from the most stable polymorphs of the pure coformers. ^[c] The root-mean-square deviations in atomic positions after optimisation was calculated by the crystal packing similarity tool in Mercury CFC 3.1⁵ with a 15 molecule comparison to the experimental structures, excluding the hydrogen atoms. ^[d] Inversion symmetry is removed to avoid unphysical conformation of the substituted dicarboxylic acid molecule.

3.0 References

1. GRACE software from Avant-garde Materials Simulation, www.avmatsim.eu.
2. G. Kresse and J. Furthmüller, *Phys. Rev. B*, 1996, **54**, 11169.
3. G. Kresse and D. Joubert, *Phys. Rev. B*, 1999, **59**, 1758.
4. M. A. Neumann and M.-A Perrin, *J. Phys. Chem. B*, 2005, **109**, 15531.
5. J. A. Chisholm and W. D. S. Motherwell, *J. Appl. Crystallogr.*, 2005, **38**, 228.
6. F. H. Allen, *Acta Crystallogr., Sect. B: Struct. Sci.*, 2002, **58**, 380.